Mineralogical Magazine, August 2017, Vol. 81(4), pp. 1001–1008

New arsenate minerals from the Arsenatnaya fumarole, Tolbachik volcano, Kamchatka, Russia. VII. Pharmazincite, $KZnAsO_4$

Igor V. Pekov[1,*], Vasiliy O. Yapaskurt[1], Dmitry I. Belakovskiy[2], Marina F. Vigasina[1], Natalia V. Zubkova[1] and Evgeny G. Sidorov[3]

[1] Faculty of Geology, Moscow State University, Vorobievy Gory, 119991 Moscow, Russia
[2] Fersman Mineralogical Museum of the Russian Academy of Sciences, Leninsky Prospekt 18-2, 119071 Moscow, Russia
[3] Institute of Volcanology and Seismology, Far Eastern Branch of the Russian Academy of Sciences, Piip Boulevard 9, 683006 Petropavlovsk-Kamchatsky, Russia

[*Received 15 March 2016; Accepted 9 September 2016; Associate Editor: Giancarlo Della Ventura*]

ABSTRACT

The new mineral pharmazincite, $KZnAsO_4$, was found in sublimates of the Arsenatnaya fumarole at the Second scoria cone of the Northern Breakthrough of the Great Tolbachik Fissure Eruption, Tolbachik volcano, Kamchatka, Russia. It is closely associated with shchurovskyite, dmisokolovite, bradaczekite, arsmirandite, tilasite, johillerite, tenorite, hematite, aphthitalite and As-bearing orthoclase. Pharmazincite occurs as prismatic to acicular crystals up to 1 mm long and up to 0.03 mm thick typically combined in near-parallel, radial or chaotic intergrowths, open-work aggregates or crusts up to 2 mm across. Pharmazincite is colourless to white, transparent, with a vitreous lustre. It is brittle, with a stepped fracture and a perfect cleavage parallel to [001]. D_{calc} is 4.75 g cm^{-3}. Pharmazincite is optically uniaxial (–), ω = 1.649(2), ε = 1.642(2). The Raman spectrum is reported. The chemical composition (wt.%, electron-microprobe data) is: K_2O 18.98, CaO 0.14, MgO 1.20, CuO 4.41, ZnO 27.58, Fe_2O_3 0.15, P_2O_5 0.50, As_2O_5 46.67, total 99.63. The empirical formula, calculated based on 4 O apfu, is: $(K_{0.97}Ca_{0.01})_{\Sigma 0.98}(Zn_{0.82}Cu_{0.13}Mg_{0.07}Fe^{3+}_{0.01})_{\Sigma 1.03}(As_{0.98}P_{0.02})_{\Sigma 1.00}O_4$. The strongest reflections of the powder X-ray diffraction pattern [*d*,Å(*I*)(*hkl*)] are: 6.36 (28)(111), 4.64(45)(220), 4.35(48)(002), 3.260(36)(411), 3.179(100)(222), 2.770(26)(113), 2.676(77)(600), 2.278(15)(602) and 1.710(15)(713, 115). Pharmazincite is hexagonal, a = 18.501(4), c = 8.7114(9) Å, V = 2582.4(8) Å^3 and Z = 24 (single-crystal XRD data). Its space group is $P6_3$, by analogy with synthetic $KZnAsO_4$ that has a crystal structure based upon a tetrahedral tridymite-type $\{ZnAsO_4\}^-$ framework. It is isostructural with megakalsilite $KAlSiO_4$. The new mineral is named for its chemical constituents.

Keywords: pharmazincite, new mineral, potassium zinc arsenate, tridymite tetrahedral framework, fumarole sublimate, Tolbachik volcano, Kamchatka.

Introduction

A unique suite of arsenate minerals was discovered at the Arsenatnaya fumarole located at the apical part of the Second scoria cone of the Northern Breakthrough of the Great Tolbachik Fissure Eruption, Tolbachik volcano, Kamchatka Peninsula, Far-Eastern Region, Russia (55°41′N 160°14′E, 1200 m asl). The description of this active fumarole, discovered by us in July 2012, is given in the first paper also containing data on the new mineral yurmarinite $Na_7(Fe^{3+},Mg,Cu)_4(AsO_4)_6$ (Pekov *et al*., 2014*a*). Later we described here two modifications of $Cu_4O(AsO_4)_2$, ericlaxmanite and kozyrevskite (Pekov *et al*., 2014*b*), popovite $Cu_5O_2(AsO_4)_2$ (Pekov *et al*., 2015*a*),

*E-mail: igorpekov@mail.ru
https://doi.org/10.1180/minmag.2016.080.146

structurally related shchurovskyite $K_2CaCu_6O_2(AsO_4)_4$ and dmisokolovite $K_3Cu_5AlO_2(AsO_4)_4$ (Pekov *et al*., 2015*b*), katiarsite $KTiO(AsO_4)$ (Pekov *et al*., 2016*a*) and melanarsite $K_3Cu_7Fe^{3+}O_4(AsO_4)_4$(Pekov *et al*., 2016*b*).

This paper reports the new mineral pharmazincite $KZnAsO_4$ (Cyrillic: фармацинкит) named for its chemical constituents, arsenic (from the Greek φαρμακου, poison) and zinc. Both the new mineral and its name have been approved by the IMA Commission on New Minerals, Nomenclature and Classification (IMA2014–015). The type specimen is deposited in the systematic collection of the Fersman Mineralogical Museum of the Russian Academy of Sciences, Moscow, under the catalogue number 94378.

Occurrence and general appearance

Specimens with the new mineral were collected by us in July 2013 from the inner, hot part of the Arsenatnaya fumarole, with temperature at the time of collecting 360–380°C (measured using a chromel-alumel thermocouple). We hypothesize that pharmazincite was deposited directly from the gas phase as a volcanic sublimate at temperatures higher than 360°C. It is a minor constituent of fumarolic incrustations also including shchurovskyite, dmisokolovite, bradaczekite, arsmirandite (IMA2014–081), tilasite, johillerite, lammerite, lammerite-β, urusovite, alarsite, ericlaxmanite, kozyrevskite, popovite, svabite, melanarsite, hatertite, yurmarinite, aphthitalite, langbeinite, calciolangbeinite, krasheninnikovite, arcanite, palmierite, steklite, dolerophanite, anhydrite, alumoklyuchevskite, vanthoffite, fluoborite, sylvite, halite, hematite, tenorite, gahnite (Cu-bearing variety), corundum, orthoclase (As-bearing variety: Koshlyakova *et al*., 2014) and fluorophlogopite.

The morphology of crystals and aggregates of pharmazincite is diverse (Figs 1 to 3). The mineral occurs as short- to long-prismatic (Fig. 1) and acicular (Fig. 2) crystals elongated along [001]. Most crystals are imperfect, with coarse striation along [001], typically skeletal, with a gear-like cross section (Fig. 3*a*, *b*); less commonly case-like individuals are observed (Fig. 3*e*). Terminations are crude, sometimes roundish (Fig. 3*c*) and/or 'fringed', with epitactic overgrowths of tiny crystals of the same mineral (Fig. 3*c*, *e*). Prismatic crystals are up to 0.03 mm × 0.07 mm while acicular crystals are up to 1 mm long and up to 0.01 mm thick. The crystals form near-parallel (Fig. 1) or chaotic clusters. Oriented intergrowths shown in Fig. 3*c* look like X-shaped twins. Open-work aggregates and crystal crusts (Figs 1 and 3*b*, *d*, *e*) up to 2 mm across and up to 0.02 mm thick were observed. The acicular crystals of pharmazincite form sprays and open-work radial aggregates up to 1.5 mm in diameter usually overgrowing crusts or dense clusters of prismatic crystals of the same mineral belonging to its earlier generation (Figs 2 and 3*f*). Pharmazincite is one of the latest minerals in the assemblage. Its crystals and aggregates occur on crusts formed by other arsenates, mainly shchurovskyite, dmisokolovite,

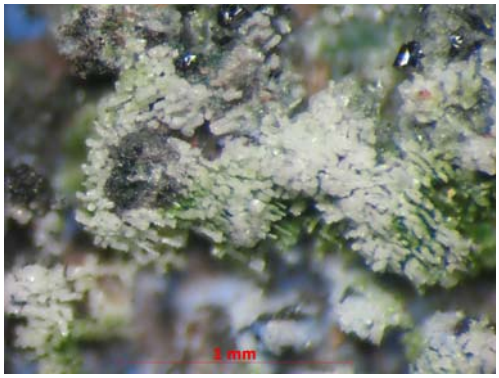

FIG. 1. Near-parallel intergrowths of colourless to white prismatic crystals of pharmazincite with green shchurovskyite, blue bradaczekite and black, metallic tenorite crystals. Field of view width: 2.1 mm. Photo: I.V. Pekov and A.V. Kasatkin.

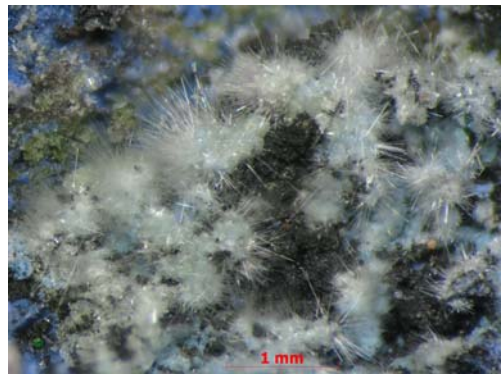

FIG. 2. Sprays and open-work radial groups of acicular crystals of pharmazincite overgrowing dense clusters of tiny prismatic crystals of the same mineral belonging to its earlier generation (both varieties are colourless to white) on a greenish-black crust of arsmirandite (IMA2014-081) with green shchurovskyite and blue bradaczekite. Field of view width: 4.4 mm. Photo: I.V. Pekov and A.V. Kasatkin.

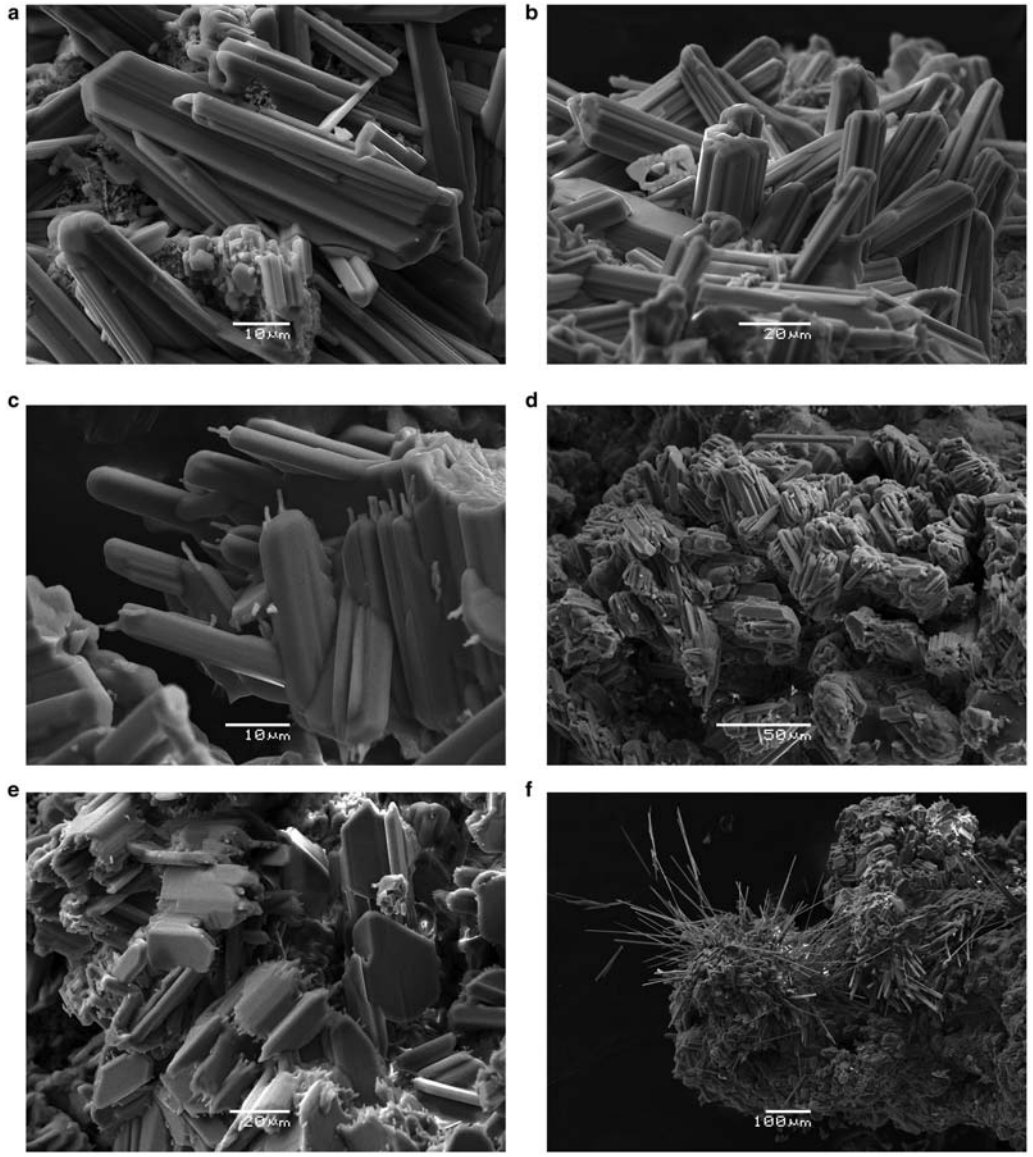

FIG. 3. Morphology of crystals and aggregates of pharmazincite: (*a*, *b*) typical skeletal, with gear-like cross-sections, prismatic crystals; (*c*) oriented intergrowths of roundly terminated coarse prismatic crystals with epitactic overgrowths of tiny prismatic crystals of the same mineral; (*d*) dense cluster of prismatic to short prismatic crystals; (*e*) crust formed by skeletal, case-like prismatic crystals with 'fringed' terminations; (*f*) acicular crystals overgrowing crusts consisting of prismatic crystals of the same mineral belonging to its earlier generation. Scanning electron microscopy secondary electron images.

tilasite (including tilasite pseudomorphs after johillerite crystals), bradaczekite and arsmirandite (Figs 1 and 2). These polycomponent arsenate incrustations cover, along with tenorite and later aphthitalite, basalt scoria altered by fumarolic gas. Areas 'sprinkled' by pharmazincite clusters are up to 1 cm × 2 cm.

Crystals of the new mineral are too small for goniometric measurements, however, based on observations under the scanning electron

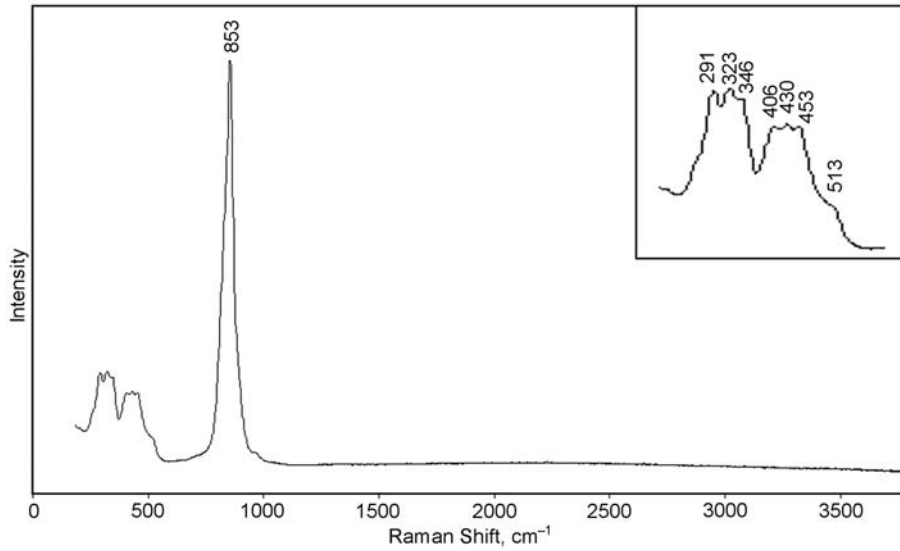

FIG. 4. The Raman spectrum of pharmazincite and an enlarged section showing the low frequency region.

microscope (Fig. 3), we assume that major crystal forms could be {110} and {101} whereas {100} and {001} are subordinate.

Physical properties and optical data

Pharmazincite is colourless in separate crystals to white in aggregates; some samples are green due to abundant micro-inclusions of Cu-rich arsenates, mainly shchurovskyite. It is transparent, with a vitreous lustre. The mineral is non-fluorescent under ultraviolet rays or an electron beam. Pharmazincite is brittle. One direction of perfect cleavage parallel to [001] and stepped fracture were observed under the microscope. Hardness and density were not measured because of the tiny size of individuals and open-work character of aggregates. The density, calculated using the empirical formula and unit-cell dimensions obtained from single-crystal X-ray diffraction data, is 4.748 g cm^{-3}.

In plane-polarized light pharmazincite is colourless and non-pleochroic. The mineral is optically uniaxial (–), ω = 1.649(2), ε = 1.642(2) (589 nm), with a negative elongation.

Raman spectroscopy

The Raman spectrum of pharmazincite (Fig. 4) was obtained on a randomly oriented crystal using an EnSpectr R532 instrument (Dept. of Mineralogy, Moscow State University) with a green laser (532 nm) at room temperature. The output power of the laser beam was ~30 mW. The spectrum was processed using the *EnSpectr* expert mode program in the range from 100 to 4000 cm^{-1} with the use of a holographic diffraction grating with 1800 lines cm^{-1} and a resolution of 5–8 cm^{-1}. The diameter of the focal spot on the sample was ~15 µm. The back-scattered Raman signal was collected with 40× objective; signal acquisition time for a single scan of the spectral range was 1500 ms and the signal was averaged over 10 scans.

A strong band at 853 cm^{-1} corresponds to As^{5+}–O stretching vibrations of AsO_4^{3-} groups. Bands with frequencies between 550 and 250 cm^{-1} correspond to As^{5+}–O bending vibrations and Zn–O stretching vibrations. An absence of bands with frequencies higher than 1000 cm^{-1} indicates the absence of groups with O–H, C–H, C–O, N–H, N–O and B–O bonds in the mineral.

Chemical composition

The chemical composition of pharmazincite was determined on a Jeol JSM-6480LV scanning electron microscope equipped with an INCA-Wave 500 wavelength-dispersive spectrometer (Laboratory of Analytical Techniques of High Spatial Resolution, Dept. of Petrology, Moscow State University), with an acceleration voltage of

TABLE 1. Powder X-ray diffraction data of pharmazincite and its synthetic analogue.

Pharmazincite			Synthetic $KZnAsO_4$: Averbuch-Pouchot and Durif (1973)		Synthetic $KZnAsO_4$: Calculated from the structure data of Colbeau-Justin (1996)		
I_{meas}	d_{meas}, Å	d_{calc}, Å	I_{meas}	d_{meas}, Å	I_{calc}	d_{calc}, Å	*hkl*
28	6.36	6.352	18	6.36	22	6.354	111
7	6.11	6.106	2	6.10	0.5	6.105	210
45	4.64	4.663	29	4.67	35	4.663	220
48	4.35	4.338	43	4.35	41	4.341	002
12	4.11	4.108	20	4.12	19	4.108	221
4	3.96	3.981	1	3.988	1	3.981	311
5	3.698	3.706, 3.661	1	3.713	1, 1	3.706, 3.661	320, 401
36	3.260	3.266	49	3.272	33	3.266	411
100	3.179	3.176	100	3.183	100	3.177	222
6	2.906	2.901	3	2.907	3	2.901	510
26	2.770	2.762	20	2.769	18	2.764	113
77	2.676	2.692	81	2.697	90	2.692	600
5	2.571	2.571	9	2.576	7	2.571	601
4	2.549	2.539	2	2.543	1	5.539	431
8	2.465	2.464, 2.458	16	2.464	3, 15	2.463, 2.459	610, 223
1	2.361	2.370	1	2.357	0.5	2.370	611
2	2.341	2.332	1	2.335	1	2.331	440
15	2.278	2.288	10	2.292	14	2.288	602
12	2.235	2.236	18	2.240	15	2.237	413
6	2.179	2.169	6	2.175	7	2.171	004
4	2.147	2.142	2	2.146	1	2.142	612
3	2.128	2.118	2	2.122	2	2.118	333
9	2.046	2.054	14	2.057	15	2.054	442
4	2.016	2.012	1	2.016	0.5	2.012	541
3	1.972	1.971	2	1.975	1	1.971	603
7	1.962	1.967	1	1.961	0.5	1.968	224
10	1.926	1.928	17	1.932	18	1.928	523
1	1.844	1.847	1	1.850	0.5	1.847	811
2	1.831	1.824	3	1.827	3	1.823	551
3	1.807	1.812, 1.804	2	1.808	1, 1	1.812, 1.804	641, 533
1	1.786	1.779	<1	1.782	1	1.779	731
15	1.710	1.720, 1.706	7	1.710	15, 5	1.720, 1.707	713, 115
7	1.690	1.689	4	1.693	4	1.690	604
2	1.674	1.676, 1.675	1	1.674	0.5, 0.5	1.676, 1.675	732, 740
11	1.627	1.633, 1.626	22	1.636	18, 8	1.633, 1.627	822, 225
3	1.613	1.618, 1.612	1	1.618	0.5, 0.5	1.619, 1.612	315, 831
2	1.580	1.582, 1.578	1	1.581	1, 1	1.583, 1.577	813, 652
11	1.555	1.557, 1.554	18	1.557	16, 19	1.558, 1.554	415, 660
8	1.541	1.547, 1.539	1	1.541	1, 1	1.547, 1.539	750, 733
3	1.533	1.533, 1.526	2	1.529	0.5, 1	1.533, 1.530	10.1.0, 840
3	1.494	1.493	1	1.496	1	1.493	930
4	1.486	1.484	<1	1.487	0.5	1.485	634
6	1.460	1.463, 1.461	14	1.466	11, 1	1.463, 1.461	662, 653
10	1.449	1.450, 1.446	7, 6	1.452, 1.444	5, 2	1.450, 1.447	743, 006
2	1.395	1.392	3	1.395	3	1.393	445
2	1.359	1.361, 1.355	2	1.357	0.5, 3	1.361, 1.355	762, 10.1.3
4	1.346	1.348, 1.346	5	1.348	2, 7	1.348, 1.346	715, 12.0.0

(continued)

TABLE 1. (*contd.*)

Pharmazincite			Synthetic $KZnAsO_4$: Averbuch-Pouchot and Durif (1973)		Synthetic $KZnAsO_4$: Calculated from the structure data of Colbeau-Justin (1996)		
I_{meas}	d_{meas}, Å	d_{calc}, Å	I_{meas}	d_{meas}, Å	I_{calc}	d_{calc}, Å	*hkl*
5	1.337	1.333, 1.332	3	1.335	1, 0.5	1.333, 1.332	942, 11.2.0
2	1.319	1.317	1	1.319	1	1.317	771
7	1.277	1.278, 1.276	3	1.277	1, 3	1.279, 1.276	815, 853
7	1.270	1.270	5	1.273	1.271		555
2	1.236	1.239, 1.236	5	1.239	6, 3	1.239, 1.237	10.4.2, 825
3	1.209	1.212, 1.210	2, 4	1.212, 1.208	1, 4	1.212, 1.210	655, 773

20 kV, a beam current of 20 nA and a 3 μm beam diameter. The following standards were used: orthoclase (K), $CaWO_4$ (Ca), olivine (Mg), $CuFeS_2$ (Cu, Fe), ZnS (Zn), GaP (P) and FeAsS (As).

The average (seven spot analyses) chemical composition of pharmazincite (wt.%, ranges are in parentheses) is: K_2O 18.98 (18.51–19.94), CaO 0.14 (0.00–0.35), MgO 1.20 (0.56–1.67), CuO 4.41 (3.05–5.73), ZnO 27.58 (25.19–30.26), Fe_2O_3 0.15 (0.00–0.54), P_2O_5 0.50 (0.18–0.95), As_2O_5 46.67 (45.74–47.57), total 99.63. Contents of other elements with atomic numbers higher than carbon were below detection limits. Admixed Fe is considered as Fe^{3+} taking into account the strongly oxidizing conditions of mineral deposition in the Arsenatnaya fumarole (Pekov *et al*., 2014*a*, 2015*b*).

The empirical formula of pharmazincite, calculated on the basis of 4 O atoms per formula unit, is: $(K_{0.97}Ca_{0.01})_{\Sigma 0.98}(Zn_{0.82}Cu_{0.13}Mg_{0.07}Fe^{3+}_{0.01})_{\Sigma 1.03}(As_{0.98}P_{0.02})_{\Sigma 1.00}O_4$. The simplified formula is $KZnAsO_4$, which requires K_2O 19.35, ZnO 33.43, As_2O_5 47.22, total 100.00 wt.%.

The Gladstone-Dale compatibility index $1 - (K_p/K_c)$ (Mandarino, 1981) is –0.038, excellent.

X-ray crystallography

The single-crystal X-ray diffraction (XRD) study of pharmazincite was carried out using an Xcalibur S diffractometer equipped with a CCD detector and gave a hexagonal unit cell with the following dimensions: a = 18.501(4), c = 8.7114(9) Å, V = 2582.4(8) Å^3 and Z = 24.

Powder XRD data for pharmazincite were collected with a STOE IPDS II single-crystal diffractometer, equipped with an Image Plate area detector, using the Gandolfi method (Mo$K\alpha$ radiation; detector-to-sample distance: 160 mm). These data are given in Table 1 in comparison with both measured and calculated powder XRD patterns of synthetic $KZnAsO_4$. Unit-cell parameters of pharmazincite refined from the powder XRD data are: a = 18.653(7), c = 8.676(6) Å and V = 2614(4) Å^3.

Discussion

The crystal structure of pharmazincite was not studied because even the best of the tested single crystals, appearing perfect, had a low quality due to its slightly divergent (micro-blocky) character. However, the powder XRD pattern of the mineral is very close in both d spacings and reflection intensities to that of synthetic $KZnAsO_4$ [hexagonal, space group $P6_3$, a = 18.6817(9), c = 8.6983(7) Å, V = 2629.0(5) Å^3 and Z = 24: Colbeau-Justin, 1996]: see Table 1. This modification is the only one known for $KZnAsO_4$. Because of the close powder XRD patterns, as well as the similarity of single-crystal XRD data and of optical uniaxiality, we conclude that pharmazincite is the natural analogue of this synthetic compound studied by Averbuch-Pouchot and Durif (1973) and by Colbeau-Justin (1996). The isostructural synthetic phosphate $KZnPO_4$ ($P6_3$, a = 18.155, c = 8.504 Å, V = 2427 Å^3 and Z = 24) is known (Andratschke *et al*., 1992).

In terms of crystal structure, $KZnAsO_4$ (Fig. 5) belongs to the family of so-called 'stuffed derivatives' of tridymite (Buerger, 1954). They are based on the tridymite-type tetrahedral framework TO_2 with a total positive charge of T < 4 that is

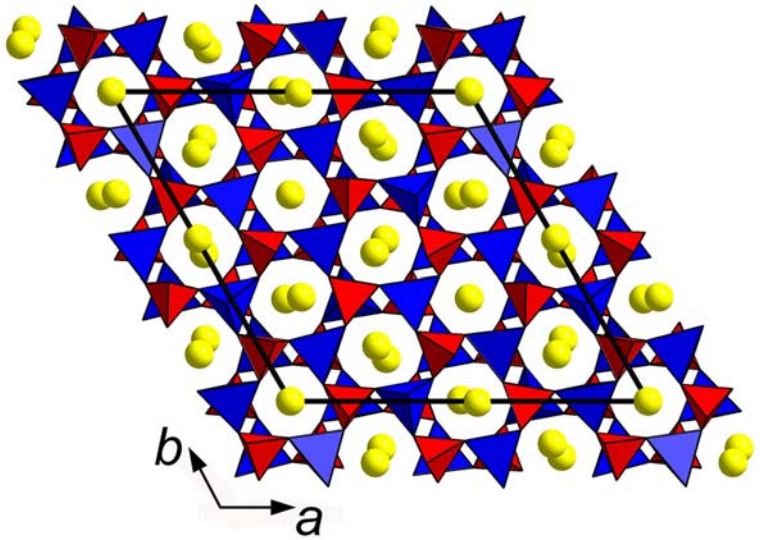

FIG. 5. The crystal structure of $KZnAsO_4$ drawn based on the data of Colbeau-Justin (1996). AsO_4 tetrahedra are red, ZnO_4 tetrahedra are blue and K atoms are yellow. The unit cell is outlined.

compensated by large cations located in voids of the framework. This family includes numerous synthetic compounds and some minerals, e.g., aluminosilicates nepheline $(Na,K)AlSiO_4$, kalsilite $KAlSiO_4$ and polymorphs of the latter (all hexagonal, $P6_3$). The structural differences between representatives of this family are caused mainly by the configuration and stacking of the tetrahedral layers forming the tridymite-type framework (Gregorkiewitz, 1986). This causes, in particular, the diversity of $KAlSiO_4$ polymorphs. $KZnAsO_4$ is isostructural with one of them, the mineral megakalsilite ($P6_3$, $a = 18.111$, $c = 8.462$ Å, $V = 2404$ Å^3 and $Z = 24$: Khomyakov *et al*., 2002), a representative of the $KAlGeO_4$ structure type (Sandomirskii *et al*., 1986). In the tetrahedral tridymite-type $\{ZnAsO_4\}^-$ framework of $KZnAsO_4$ (Colbeau-Justin, 1996), As and Zn atoms occupy positions corresponding to positions of Al and Si, respectively, in megakalsilite.

Acknowledgements

We thank Natale Perchiazzi and anonymous reviewer for valuable comments. This study was supported by the Russian Science Foundation, grant no. 14-17-00048. The technical support by the SPbSU X-Ray Diffraction Resource Center in the XRD powder-diffraction studies is acknowledged.

References

Andratschke, M., Range, K.J., Haase, H. and Klement, U. (1992) Die Kristallstruktur von α-$KZnPO_4$. *Zeitschrift für Naturforschung, Teil B. Anorganische Chemie, organische Chemie*, **47**, 1249–1254.

Averbuch-Pouchot, M.T. and Durif, A. (1973) Donnees cristallographiques sur $ZnKPO_4$ et $ZnKAsO_4$. *Materials Research Bulletin*, **8**, 353–356.

Buerger, M.J. (1954) The stuffed derivatives of the silica structures. *American Mineralogist*, **39**, 600–614.

Colbeau-Justin, C. (1996) *Cristallochimie et proprietes non linearies de nouveaux composes a structures cristobalite et tridymite deformees*. PhD thesis, Universit de Paris 6, Paris.

Gregorkiewitz, M. (1986) Alkali ion diffusion in M ($AlSiO_4$) compounds with frameworks of the tridymite topology and its variations. *Solid State Ionics*, **18–19**, 534–538.

Khomyakov, A.P., Nechelyustov, G.N., Sokolova, E.V., Bonaccorsi, E., Merlino S. and Pasero, M. (2002) Megakalsilite, a new polymorph of $KAlSiO_4$ from the Khibina massif, Kola Peninsula, Russia: mineral description and crystal structure. *The Canadian Mineralogist*, **40**, 961–970.

Koshlyakova, N.N., Pekov, I.V., Yapaskurt, V.O. and Sidorov, E.G. (2014) Arsenic-bearing potassic feldspar – a product of fumarolic exhalations and gas metasomatism at the Tolbachik volcano (Kamchatka, Russia). Pp. 55–56 in: *International Conference "Ore Potential of Alkaline, Kimberlite and Carbonatite Magmatism"*, GEOKHI RAS, Moscow.

Mandarino, J.A. (1981) The Gladstone-Dale relationship. Part IV. The compatibility concept and its application. *The Canadian Mineralogist*, **14**, 498–502.

Pekov, I.V., Zubkova, N.V., Yapaskurt, V.O., Belakovskiy, D.I., Lykova, I.S., Vigasina, M.F., Sidorov, E.G. and Pushcharovsky, D.Yu. (2014*a*) New arsenate minerals from the Arsenatnaya fumarole, Tolbachik volcano, Kamchatka, Russia. I. Yurmarinite, $Na_7(Fe^{3+}, Mg,Cu)_4(AsO_4)_6$. *Mineralogical Magazine*, **78**, 905–917.

Pekov, I.V., Zubkova, N.V., Yapaskurt, V.O., Belakovskiy, D.I., Vigasina, M.F., Sidorov, E.G. and Pushcharovsky, D.Yu. (2014*b*) New arsenate minerals from the Arsenatnaya fumarole, Tolbachik volcano, Kamchatka, Russia. II. Ericlaxmanite and kozyrevskite, two natural modifications of $Cu_4O(AsO_4)_2$. *Mineralogical Magazine*, **78**, 1527–1543.

Pekov, I.V., Zubkova, N.V., Yapaskurt, V.O., Belakovskiy, D.I., Vigasina, M.F., Sidorov, E.G. and Pushcharovsky, D.Yu. (2015*a*) New arsenate minerals from the Arsenatnaya fumarole, Tolbachik volcano, Kamchatka, Russia. III. Popovite, $Cu_5O_2(AsO_4)_2$. *Mineralogical Magazine*, **79**, 133–143.

Pekov, I.V., Zubkova, N.V., Belakovskiy, D.I., Yapaskurt, V.O., Vigasina, M.F., Sidorov, E.G. and Pushcharovsky, D.Yu. (2015*b*) New arsenate minerals from the Arsenatnaya fumarole, Tolbachik volcano, Kamchatka, Russia. IV. Shchurovskyite, $K_2CaCu_6O_2(AsO_4)_4$ and dmisokolovite, $K_3Cu_5AlO_2(AsO_4)_4$. *Mineralogical Magazine*, **79**, 1737–1753.

Pekov, I.V., Yapaskurt, V.O., Britvin, S.N., Zubkova, N.V., Vigasina, M.F. and Sidorov, E.G. (2016*a*) New arsenate minerals from the Arsenatnaya fumarole, Tolbachik volcano, Kamchatka, Russia. V. Katiarsite, $KTiO(AsO_4)$. *Mineralogical Magazine*, **80**, 639–646.

Pekov, I.V., Zubkova, N.V., Yapaskurt, V.O., Polekhovsky, Yu.S., Vigasina, M.F., Belakovskiy, D.I., Britvin, S.N., Sidorov, E.G. and Pushcharovsky, D.Yu. (2016*b*) New arsenate minerals from the Arsenatnaya fumarole, Tolbachik volcano, Kamchatka, Russia. VI. Melanarsite, $K_3Cu_7Fe^{3+}O_4(AsO_4)_4$. *Mineralogical Magazine*, **80**, 855–867.

Sandomirskii, P.A., Meshalkin, S.S., Rozhdestvenskaya, I.V., Dem'yanets, L.N. and Uvarova, T.G. (1986) Crystal structures of the *D*-phase of $KAlGeO_4$ and the *C*-phase of $NaAlGeO_4$. *Soviet Physics, Crystallography*, **31**, 522–527.